Stabilization of dispersion-managed solitons in random optical fibers by strong dispersion management

J. Garnier
Laboratoire de Statistique et Probabilités,
Université Paul Sabatier, 118 Route de Narbonne, 31062 Toulouse Cedex 4, France,
Tel. (33) 5 61 55 62 20, Fax. (33) 5 61 55 60 89, Email: garnier@cict.fr
(March 27, 2002)

The propagation of dispersion-managed solitons in optical fibers with randomly perturbed dispersion maps is considered. The interplay between the periodic dispersion management and the random dispersive fluctuations is precisely analyzed. Analytic expressions are derived for the moments of the pulse widths as well as for the probability density functions. It is shown that a strong dispersion management stabilizes the soliton, while a small anomalous residual dispersion is necessary for preventing from a stochastic resonance phenomenon. Analytical results are confirmed by direct numerical simulations.
Keywords. Dispersion-managed soliton, random dispersion.

I. INTRODUCTION

The dispersion management (DM) technique for short pulse propagation in optical fibers has become a subject of great interest for telecommunication applications [1–3]. Indeed the main limitation of high-bit rate transmission in optical fiber links is the chromatic dispersion. Other limitations are fiber loss, radiation from the pulse due to lumped amplifiers compensating the fiber loss [4], noise and the Gordon-Haus effect resulting from the interaction with noise [5], and other nonlinear effects (modulational instability [6], jitters caused by collisions between signals [7],...). Two solutions have been proposed to compensate for the pulse broadening induced by dispersion. The first solution is the soliton transmission, where the dispersion is balanced by the Kerr nonlinearity [8]. One of the main drawbacks is that four-wave mixing has been shown to be detrimental for wavelength-division multiplexing in a conventional soliton transmission line [9]. The second solution is a direct dispersion compensation for linear pulse propagation by the use of a periodic concatenation of pieces of fibers with opposite signs of dispersion [10]. However in any realistic optical network it will not be possible to compensate for all the dispersion in each element, so that there will remain some residual dispersion. Furthermore the amplitude of the signal is bounded from below to keep a reasonable signal-to-noise ratio, so that the nonlinearity should be also taken into account. It was shown that the pulse propagation in such conditions was described by the nonlinear Schrödinger equation with a distance-varying dispersion coefficient [3]. As a result the concept of DM soliton in dispersion compensated lines was proposed. It combines the advantages of the traditional fundamental soliton of the nonlinear Schrödinger equation, and the dispersion-managed signal transmission. Both computational and experimental investigations have shown the existence and the stability of this new type of optical solitary wave. However the theoretical understanding of the DM soliton is still far from being complete (see [11] for a review). Furthermore it is well known that the nonlinear Schrödinger equation does not completely describe the pulse propagation in realistic fiber transmission links. In addition to the periodic dispersion management and nonlinearity, random fluctuations of dispersion may occur [12,13]. Indeed recent measurements by a reflectometer yield the significance of dispersion randomness [14,15]. These terms have been shown to involve dramatic effects on the modulational instability of stationary waves because of a stochastic parametric resonance phenomenon [16]. In this paper we shall analyze the stability of the DM soliton with respect to random fluctuations of the dispersion.

II. FORMULATION

The optical pulse propagation in a system with varying dispersion is governed by the nonlinear Schrödinger (NLS) equation [17]:

$$iE_Z - \frac{1}{2}\beta_2(Z)E_{TT} + \sigma_{nl}|E|^2E = 0, \tag{1}$$

where Z is the propagation distance (in km), T is the time in the frame moving with the group velocity (in ps), $P = |E|^2$ is the optical power (in W), β_2 is the group velocity dispersion coefficient (in ps^2/km). The coefficient β_2 is related to the usual dispersion parameter D by $\beta_2 = -\lambda_0^2 D/(2\pi c)$ where $c = 0.3$ mm/ps is the speed of light, λ_0 is the carrier wavelength (in μm), and D is measured in ps/nm/km. The pulse energy is independent of Z:

$$\mathcal{E}_{\rm pulse} = \int |E|^2(Z,T)DT.$$

The carrier wavelength is $\lambda_0 = 1.55$ μm for telecommunication applications. The nonlinear coefficient $\sigma_{nl} = 2\pi n_2/(\lambda_0 A_{\rm eff})$ (in W^{-1}m^{-1}) where n_2 is the nonlinear refractive index ($n_2 = 3\ 10^{-2}$ nm^2/W in glass) and $A_{\rm eff}$ is the effective fiber area (in μm^2). Typically $A_{\rm eff} \simeq 60$ μm^2.

It should be mentioned that in real fiber systems there is loss and periodic amplification compensating the fiber loss. If the dispersion compensation period is much larger than the amplification distance, then the technique of guiding center soliton or loss averaging can be applied to get the effective loss-free NLS equation [18,19]. This model is well justified in the long-haul transmission systems.

We introduce the typical nonlinear length $Z_0 := 1/(\sigma_{nl}P_0)$ where P_0 is the typical pulse power. In most practical applications P_0 is equal to a few milliwatts. Say $P_0 = 2\ 10^{-3}$W, so that $Z_0 = 250$ km. We normalize the coordinate along the fiber $z = Z/Z_0$ and the envelope of the electric field $u = E/\sqrt{P_0}$. We also normalize the time $t = T/T_0$ where T_0 is the typical pulse width T_0, say $T_0 = 5$ ps, so that the propagation is governed by the dimensionless nonlinear Schrödinger equation:

$$iu_z + \frac{d(z)}{2}u_{tt} + |u|^2u = 0,$$

where

$$d(z) = -\beta_2(Z_0 z) Z_0 / T_0^2 = \lambda_0^2 D(Z_0 z) Z_0 / (2\pi c T_0^2).$$

Let us assume that the group velocity dispersion (GVD) coefficient has periodic variations such as the ones described in Fig. 1, where the period is $L_{\rm map} = L_- + L_+$. Our analysis is based on the separation of the scales $L_{\rm map} \ll Z_0$. In the first part of this paper we shall study a pure periodic dispersion management. Thus we shall assume a physical dispersion management of the type:

$$D(Z) = \begin{cases} D_+ \text{ if } Z \bmod L_{\rm map} \in [0, L_+/2), \\ D_- \text{ if } Z \bmod L_{\rm map} \in [L_+/2, L_{\rm map} - L_+/2), \\ D_+ \text{ if } Z \bmod L_{\rm map} \in [L_{\rm map} - L_+/2, L_{\rm map}), \end{cases}$$

whose mean dispersion is $D_m = (D_+ L_+ + D_- L_-)/L_{\rm map}$. In dimensionless units the GVD coefficient d is of the form $d(z) = d_0(z) + d_1(z)$ where d_0 is the zero-mean dispersion compensation

$$d_0(z) = \begin{cases} d_+ \text{ if } z \bmod l_{\rm map} \in [0, l_+/2), \\ d_- \text{ if } z \bmod l_{\rm map} \in [l_+/2, l_{\rm map} - l_+/2), \\ d_+ \text{ if } z \bmod l_{\rm map} \in [l_{\rm map} - l_+/2, l_{\rm map}), \end{cases}$$

$l_{\rm map} = L_{\rm map}/Z_0$, $l_\pm = L_\pm/Z_0$, $d_\pm = \lambda_0^2 (D_\pm - D_m) Z_0/(2\pi c T_0^2)$, and d_1 is simply the mean residual dispersion $d_m = \lambda_0^2 D_m Z_0/(2\pi c T_0^2)$. The so-called dispersion management (DM) strength is

$$D_L := d_+ l_+ = -d_- l_-.$$

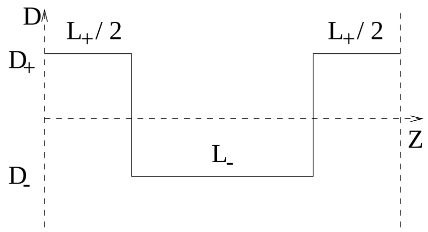

FIG. 1. Typical dispersion map.

The second part of the paper is devoted to a study of random dispersive fluctuations on the pulse propagation in DM systems. We shall assume that $d(z) = d_0(z) + d_1(z)$ where d_0 corresponds to the zero-mean periodic map and d_1 contains both the mean residual dispersion as well as the random dispersive fluctuations.

A. Soliton dynamics

The first step of the approach is based on previous work. It consists in reducing the partial differential equation to a finite-dimensional problem by deriving a set of ordinary differential equations for the pulse parameters. Following [20] we introduce the rms pulse width and the rms chirp of the pulse:

$$T_{rms} = \left(\frac{\int t^2 |u|^2 dt}{\int |u|^2 dt} \right)^{1/2},$$

$$\frac{M_{rms}}{T_{rms}} = \frac{i}{4} \frac{\int t(u u_t^* - u^* u_t) dt}{\int t^2 |u|^2 dt}.$$

By assuming that the pulse has a self-similar structure, at least in the energy bearing part :

$$u(z,t) = Q\left(\frac{t}{a(z)}\right) \exp\left(i \frac{b(z)}{a(z)} \frac{t^2}{2} \right),$$

Turitsyn [20] derives a closed-form system of ordinary differential equations for T_{rms} and M_{rms}, or alternatively a and b since both pairs are related to each other through the identities:

$$\frac{a(z)}{a(0)} = \frac{T_{rms}(z)}{T_{rms}(0)},$$
$$\frac{b(z)}{a(z)} = \frac{M_{rms}(z)}{T_{rms}(z)}.$$

The system at hand can be written in the form:

$$\frac{da}{dz} = d(z)b,$$
$$\frac{db}{dz} = \frac{C_1 d(z)}{a^3} - \frac{2C_2\mathcal{E}}{a^2},$$

where $\mathcal{E}$ is the (dimensionless) pulse energy:

$$\mathcal{E} = \int |u|^2 dt = \frac{\mathcal{E}_{\text{pulse}}}{P_0 T_0},$$

and the constants C_1 and C_2 depend only on the shape function Q:

$$C_1 = \frac{\int |Q_s|^2 ds}{\int s^2 |Q|^2 ds},$$
$$C_2 = \frac{\int |Q|^4 ds}{\left(\int s^2|Q|^2 ds\right) . \left(\int |Q|^2 ds\right)}.$$

For the Gaussian approximation of the pulse function we have:

$$C_1 = 4, \qquad C_2 = \pi^{-1/2}.$$

Throughout the paper the theoretical results will be derived with the Gaussian ansatz so that the considered system is:

$$\frac{da}{dz} = d(z)b, \tag{2a}$$
$$\frac{db}{dz} = \frac{4d(z)}{a^3} - \frac{2C_E}{a^2}, \tag{2b}$$

where $C_E = \mathcal{E}/\sqrt{\pi}$. Note that this system was first derived by applying the variational approach [22,23].

B. Separation of scales

We denote $D_0(z) = \int_0^z d_0(s)ds$ (which is a periodic function with period l_{map}) and we introduce the periodic orbits $\mathcal{A}(a_0, b_0, z)$ and $\mathcal{B}(a_0, b_0, z)$:

$$\mathcal{A}(a_0, b_0, z) = \sqrt{a_0^2 + 2a_0 b_0 D_0(z) + \left(b_0^2 + 4a_0^{-2}\right) D_0(z)^2},$$
$$\mathcal{B}(a_0, b_0, z) = \frac{a_0 b_0 + \left(b_0^2 + 4a_0^{-2}\right) D_0(z)}{\sqrt{a_0^2 + 2a_0 b_0 D_0(z) + \left(b_0^2 + 4a_0^{-2}\right) D_0(z)^2}}.$$

If $C_E = 0$ and $d_1 \equiv 0$, then $a(z) = \mathcal{A}(z)$ and $b(z) = \mathcal{B}(z)$ are the solutions of system (2) starting from (a_0, b_0).

More generally, denoting by X the row vector (a, b), we can write system (2) as:

$$\frac{dX}{dz} = F(X)d_0(z) + G(X, z),$$

where

$$F(a, b) = \begin{pmatrix} b \\ 4a^{-3} \end{pmatrix},$$
$$G(a, b, z) = \begin{pmatrix} d_1(z)b \\ 4d_1(z)a^{-3} - 2C_E a^{-2} \end{pmatrix}.$$

Our forthcoming analysis is based on a technique of separation of scales. We assume that the variations of the coefficients a and b over a period $l_{\rm map}$ involved by d_1 and C_E are small. So the short scale dynamics of the parameters (a, b) is driven by d_0 and follows the periodic orbits $(\mathcal{A}, \mathcal{B})$. Further the long-scale dynamics of the parameters (a, b) are driven by an effective system where the fast periodic oscillations have been averaged. The derivation of this effective system is performed in Appendix A. The main result can be formulated as follows. Denote:

$$M(a,b,s) = \begin{pmatrix} \frac{\partial \mathcal{A}}{\partial a}(a,b,s) & \frac{\partial \mathcal{A}}{\partial b}(a,b,s) \\ \frac{\partial \mathcal{B}}{\partial a}(a,b,s) & \frac{\partial \mathcal{B}}{\partial b}(a,b,s) \end{pmatrix}$$

and

$$\begin{pmatrix} f_a(a,b,z) \\ f_b(a,b,z) \end{pmatrix} = \left\langle M^{-1}(a,b,.)G(\mathcal{A}(a,b,.),\mathcal{B}(a,b,.),.)\right\rangle_{\rm map},$$

where $\langle . \rangle_{\rm map}$ stands for an averaging over the local map that contains z:

$$\langle \phi(.) \rangle_{\rm map}(z) := \frac{1}{l_{\rm map}} \int_0^{l_{\rm map}} \phi([z/l_{\rm map}]l_{\rm map} + \zeta) d\zeta.$$

The solution (a, b) of system (2) can be written as:

$$a(z) = \mathcal{A}(\bar{a}(z), \bar{b}(z), z), \tag{3a}$$

$$b(z) = \mathcal{B}(\bar{a}(z), \bar{b}(z), z), \tag{3b}$$

where $(\bar{a}, \bar{b})$ obeys the effective system:

$$\frac{d\bar{a}}{dz} = f_a(\bar{a}, \bar{b}, D_1(z)), \tag{4a}$$

$$\frac{d\bar{b}}{dz} = f_b(\bar{a}, \bar{b}, D_1(z)), \tag{4b}$$

and D_1 is the average dispersion over the $[z/l_{\rm map}]$-th span:

$$D_1(z) = \frac{1}{l_{\rm map}} \int_0^{l_{\rm map}} d_1([z/l_{\rm map}]l_{\rm map} + \zeta) d\zeta.$$

In absence of random fluctuations, D_1 is constant and equal to the mean residual dispersion. System (4) governs the long-scale dynamics of the parameters of the DM soliton, while system (3) describes their fast periodic oscillations.

The functions f_a and f_b are parametrized by the dispersion strength D_L, the residual dispersion d_m, and the energy coefficient C_E. The complete expressions are written in Appendix B. Note that the functions f_j's are of the form:

$$f_a(a,b,d_m) = C_E F_a\left(a\frac{C_E}{d_m}, b\frac{d_m}{C_E}, D_L\frac{C_E^2}{d_m^2}\right),$$

$$f_b(a,b,d_m) = \frac{C_E^3}{d_m^2} F_b\left(a\frac{C_E}{d_m}, b\frac{d_m}{C_E}, D_L\frac{C_E^2}{d_m^2}\right),$$

where $(A, B, D) \mapsto F_j(A, B, D)$ are dimensionless. Accordingly the dispersion strength should be measured as a function of $D_L C_E^2/d_m^2$. If $D_L \ll d_m^2/C_E^2$, then the f_j's can be expanded as $f_a(a, b, d_m) = d_m b$ and $f_b(a, b, d_m) = (4d_m - 2C_E a)/a^3$ and we get back the homogeneous functions of system (2). In this limit the problem can be regarded as a particular case of the Kepler problem [24]. On the contrary when $D_L \gg d_m^2/C_E^2$ the dispersion management will play a primary role in the long-scale dynamics of the soliton parameters.

III. THE STATIONARY POINT

Assume a pure periodic dispersion management so that $d_1(z) \equiv d_m$. We are looking for stationary configurations, that is to say pairs of values (a_s, b_s) such that $\bar{a}(z) \equiv a_s$ and $\bar{b}(z) \equiv b_s$, which also reads as $f_a(a_s, b_s, d_m) = f_b(a_s, b_s, d_m) = 0$. By studying the function f_a one can see that it vanishes for $b = 0$, whatever a. So the problem is reduced to find the chirp free stationary points, i.e. the values a_s at which $f_b(a_s, 0, d_m) = 0$.

A. Positive (anomalous) mean dispersion

If $d_m > 0$ then there exists a unique stationary point for which $\bar{b} \equiv 0$ and $\bar{a} \equiv a_s$ that satisfies $f_b(a_s, 0, d_m) = 0$. This equation also reads as:

$$a_s = \frac{d_m}{C_E} A_s \left(D_L \frac{C_E^2}{d_m^2} \right) , \tag{5}$$

where $D \mapsto A_s(D)$ is the unique solution of:

$$A_s^3 \sqrt{D^2 + A_s^4} \ln \left(\frac{\sqrt{D^2 + A_s^4} + D}{\sqrt{D^2 + A_s^4} - D} \right) + 4D \left(\sqrt{D^2 + A_s^4} - A_s^3 \right) = 0. \tag{6}$$

For weak DM the stationary point a_s can be expanded as powers of $C_E^2 d_m^{-2} D_L$:

$$a_s \overset{D_L \ll d_m^2/C_E^2}{\simeq} \frac{2d_m}{C_E} \left(1 + \frac{5C_E^4}{96 d_m^4} D_L^2 + O(\frac{C_E^8}{d_m^8} D_L^4) \right) ,$$

while for strong DM we have:

$$a_s \overset{D_L \gg d_m^2/C_E^2}{\simeq} \alpha_s \sqrt{D_L} \left(1 + \beta_s \frac{d_m}{C_E \sqrt{D_L}} + O(\frac{d_m^2}{C_E^2 D_L}) \right) , \tag{7}$$

where $\alpha_s \simeq 0.548835$ is the solution of:

$$\sqrt{1 + \alpha_s^4} \ln \left(\frac{\sqrt{1 + \alpha_s^4} + 1}{\sqrt{1 + \alpha_s^4} - 1} \right) = 4,$$

and $\beta_s = \frac{(1+\alpha_s^4)^{3/2}}{(1-\alpha_s^4)\alpha_s^3} \simeq 7.58$.

Remark 1. One should be cautious when applying the asymptotic formula (7) as D_L needs to be much larger (by a factor $\geq 10^3$) than d_m^2/C_E^2 so that the identity holds true. When the ratio $D_L C_E^2/d_m^2$ is equal to a few tens (which is very standard for telecommunication applications) one should compute the true solution of Eqs. (5)-(6). The stationary point is plotted in Figure 2 as a function of the DM strength for the case $d_m = 1$, $C_E = 1$.

To sum-up: the stationary point a_s corresponds to strictly periodic variations of the amplitude, width and chirp of the DM soliton. The stationary point is all the larger (which corresponds to a wider soliton) as D_L is large. The existence of this point has first been obtained in [21]. The contribution of our paper consists in a thorough analysis of the stability of this point. One should first study the linear stability of this point.

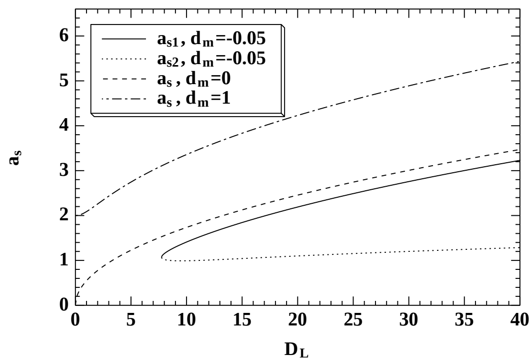

FIG. 2. Stationary point a_s as a function of the dispersion strength D_L for $d_m = -0.05$ (two stationary points $a_{s,1}$ and $a_{s,2}$) $d_m = 0$, and $d_m = 1$. Here we take $C_E = 1$.

Linear stability analysis. Assume $a = a_s + \varepsilon a_1$, $b = \varepsilon b_1$ substitute into Eq. (4), and collect the terms of order ε:

$$\frac{da_1}{dz} = \partial_b f_a b_1, \tag{8a}$$
$$\frac{db_1}{dz} = \partial_a f_b a_1, \tag{8b}$$

where we have denoted:

$$\partial_b f_a = \frac{\partial f_a}{\partial b}(a_s, 0, d_m), \tag{9a}$$
$$\partial_a f_b = \frac{\partial f_b}{\partial a}(a_s, 0, d_m). \tag{9b}$$

The partial derivatives $\frac{\partial f_a}{\partial a}(a_s, 0, d_m)$ and $\frac{\partial f_b}{\partial b}(a_s, 0, d_m)$ are zero, while $\partial_b f_a$ and $\partial_a f_b$ read as:

$$\partial_b f_a = d_m G_a \left(D_L \frac{C_E^2}{d_m^2} \right),$$
$$\partial_a f_b = \frac{C_E^4}{d_m^3} G_b \left(D_L \frac{C_E^2}{d_m^2} \right),$$

where $D \mapsto G_j(D)$ are dimensionless:

$$G_a(D) = \frac{A_s^7(D)}{2(D^2 + A_s^4(D))^{3/2}}, \tag{10a}$$
$$G_b(D) = \frac{4(A_s^4(D) - D^2)}{A_s(D)(D^2 + A_s^4(D))^{3/2}} - \frac{12}{A_s^4(D)}. \tag{10b}$$

The point $(a_s, 0)$ is stable if and only if $\gamma \geq 0$ where

$$\gamma := -\partial_b f_a \partial_a f_b. \tag{11}$$

A study of this function shows that it is always the case since $\partial_b f_a > 0$ and $\partial_a f_b < 0$ (if $d_m \geq 0$). The function γ is of the form:

$$\gamma = \frac{C_E^4}{d_m^2} \Gamma \left(D_L \frac{C_E^2}{d_m^2} \right).$$

where $D \mapsto \Gamma(D) := -G_a G_b(D)$ is dimensionless. For weak DM, we have

$$\gamma \overset{D_L \ll d_m^2/C_E^2}{\simeq} \frac{C_E^4}{4 d_m^2} \left(1 - \frac{1}{24} \frac{C_E^4}{d_m^4} D_L^2 + O(\frac{C_E^8}{d_m^8} D_L^4) \right).$$

For strong DM:

$$\gamma \overset{D_L \gg d_m^2/C_E^2}{\simeq} C_E^2 \frac{2\alpha_s^6(1-\alpha_s^4)}{(1+\alpha_s^4)^3} D_L^{-1} \simeq 3.8\, 10^{-2} C_E^2 D_L^{-1}.$$

γ is an important parameter. It characterizes the secondary oscillations of the DM soliton. Indeed if the input pulse is exactly the DM soliton defined as the periodic solution of the partial differential equation, then no oscillation is noticeable. However, if the input pulse is not strictly equal to the DM soliton, which is always the case in experiments, or else if the parameters of the dispersion map randomly fluctuate around the ideal periodic modulations, then the chirp and the width of the soliton will experience oscillations along propagation with a characteristic period equal to $2\pi/\sqrt{\gamma}$. Finally periodic secondary oscillations are important from the point of view of the stability with respect to random perturbations since a stochastic resonance phenomenon is then likely. This issue will be discussed in Section IV E.

B. Negative (normal) mean dispersion

If $d_m < 0$, then there exists no stationary point if $D_L C_E^2 d_m^{-2} < D_c$, $D_c \simeq 3102.2$.
If $D_L C_E^2 d_m^{-2} > D_c$ then there exist two stationary points $a_{s,1} > a_{s,2}$ that satisfy $f_b(a_{s,j}, 0, d_m) = 0$. This equation also reads as:

$$a_{s,j} = \frac{|d_m|}{C_E} A_{s,j} \left(D_L \frac{C_E^2}{d_m^2} \right), \tag{12}$$

where $D \mapsto A_{s,j}(D)$, $j = 1, 2$, are the two solutions (with $A_{s,1} > A_{s,2}$) of:

$$a_s^3 \sqrt{D^2 + a_s^4} \ln \left(\frac{\sqrt{D^2 + a_s^4} + D}{\sqrt{D^2 + a_s^4} - D} \right) - 4D \left(\sqrt{D^2 + a_s^4} + a_s^3 \right) = 0. \tag{13}$$

The stationary points $a_{s,1}$ and $a_{s,2}$ are plotted in Figure 2 for $d_m = -0.05$ and $C_E = 1$. An alternative graphic representation that is maybe more standard consists in plotting the stationary point (proportional to the pulse rms width) as a function of the mean dispersion (Figure 3). Note that in case of strong DM we have:

$$a_{s,1} \overset{D_L \gg d_m^2/C_E^2}{\simeq} \alpha_s \sqrt{D_L} \left(1 + \beta_s \frac{d_m}{C_E \sqrt{D_L}} + O(\frac{d_m^2}{C_E^2 D_L}) \right)$$

Linear stability analysis. Performing the same study as in the case $d_m > 0$, we put into evidence that $a_{s,2}$ is unstable, while $a_{s,1}$ is stable. The corresponding coefficient γ_1 is positive. For strong dispersion management $D_L \gg d_m^2 C_E^{-2}$, it is equal to:

$$\gamma_1 \overset{D_L \gg d_m^2/C_E^2}{\simeq} C_E^2 \frac{2\alpha_s^6 (1 - \alpha_s^4)}{(1 + \alpha_s^4)^3} D_L^{-1} \simeq 3.8\, 10^{-2} C_E^2 D_L^{-1}.$$

The existence of two possible DM soliton solutions in the normal mean dispersion regime was first pointed out in [25]. The linear stability analysis shows that only one of these solutions is actually stable. Nevertheless the coefficient $-\gamma_2$ that governs the instability growth of the second solution can be small in some configurations, so that the second DM soliton solution can be observed during several maps.

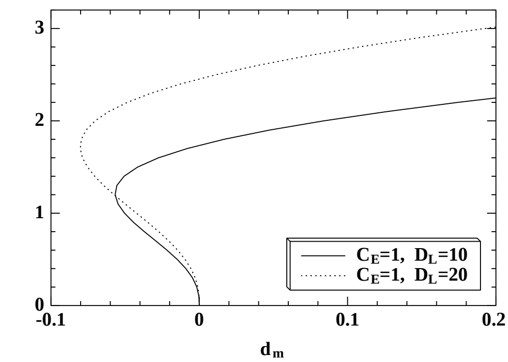

FIG. 3. Stable stationary point $a_s = a_{s,1}$ as a function of the dispersion strength D_L for $d_m = -0.05$ and $C_E = 1$.

C. Some remarks

The criterion for the existence of a stable stationary point is:

$$d_m > -C_E^{-1} \sqrt{D_c / D_L}.$$

where $D_c = 3102.2$. Note that the zero mean dispersion case, which was not specifically addressed in the previous sections, can be regarded as a limit case of the positive mean dispersion case or else of the negative mean dispersion case. In this configuration, the critical point is $a_s = \alpha_s \sqrt{D_L}$ independent of C_E.

D. Numerical simulations

A numerical routine that converges to the DM soliton is the following [26]. Consider a dispersion map with DM strength D_L and mean dispersion d_m and fix the pulse energy. Compute from Eq. (5) the stationary point a_s corresponding to this set of parameters. The point a_s is the half rms width of the Gaussian pulse that should be stable according to the ansatz approach. Launch this chirp free Gaussian pulse E in the system at the middle of the first span of the map. The pulse will show small secondary oscillations in the slow dynamics, since the Gaussian ansatz is not perfect. Record the pulse width periodically at the midpoint of each first span, and find the pulses for which the pulse widths are minimal or maximal, $E_{min}(t)$ and $E_{max}(t)$ respectively. Add them so that their tops are in phase, and rescale the resulting profile to the original pulse energy. Start again with the new E. This procedure lead to an exactly periodic solution in a few steps, unless the nonlinearity is too small (in which case the convergence takes longer) or too large (in which case the convergence does not occur because of instabilities). This solution is a periodic solution of the partial differential equation. It possesses exactly the input energy of the theoretical Gaussian pulse. It is the true DM soliton. We can then compare the rms widths of the DM solitons with the ones of the Gaussian pulses that are theoretically predicted for different configurations.

Positive mean dispersion. Tables I-II show that the formula which derives from the ansatz approach and the separation of scales technique efficiently predicts the rms widths of the DM solitons in case of positive mean dispersion, since the departures between the theoretically predicted rms widths and the real ones are below 1 %. The theoretical values are $T_{rmstheo} = a_s/2$ where a_s is computed from Eqs. (5-6). For consistency we also plot in Figure 4 the power profiles of the DM solitons. The energy bearing parts of the profiles are very close to the theoretical Gaussian profiles, although the tails may be different.

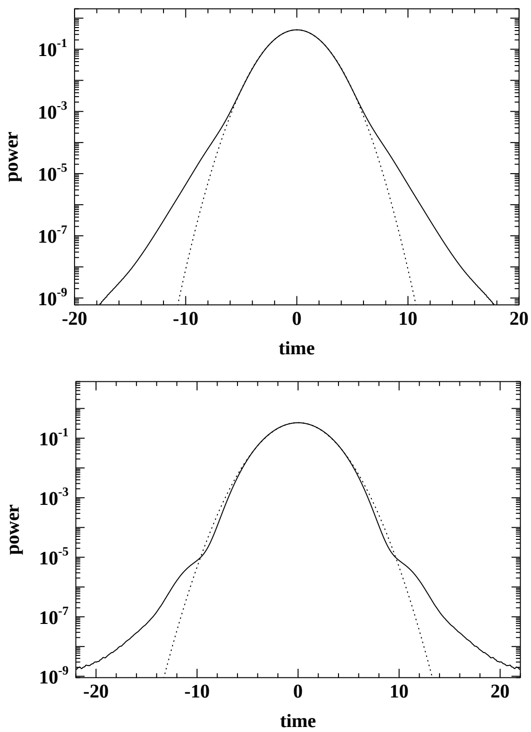

(a) (b)

FIG. 4. Power profiles of the DM solitons determined by numerical simulations of the NLS equation (solid lines) compared with the theoretically predicted Gaussian pulses (dotted lines). Here $d_m = 1$, $C_E = 1$, $l_+ = l_- = 0.1$, $D_L = 10$ (a), and $D_L = 20$ (b).

Zero-mean dispersion. Consider now the two typical zero-mean dispersion configurations proposed in Tables III-IV. The theoretical values are here simply $T_{rmstheo} = a_s/2 = \alpha_s\sqrt{D_L}/2$. The departures between the theoretical and numerical values of the rms widths are of the order of 5 %, which is more important than in the positive mean dispersion regime. This is due to the fact that the self-similar structure of the DM soliton is here sensibly different from a Gaussian shape that is assumed throughout the theoretical study. We should gain precision by adjusting the theory with more accurate values for the shape parameters C_1 and C_2. However we are willing to propose an approach without any free parameter that should be fixed by the user. Note that the results are still very good with the Gaussian ansatz.

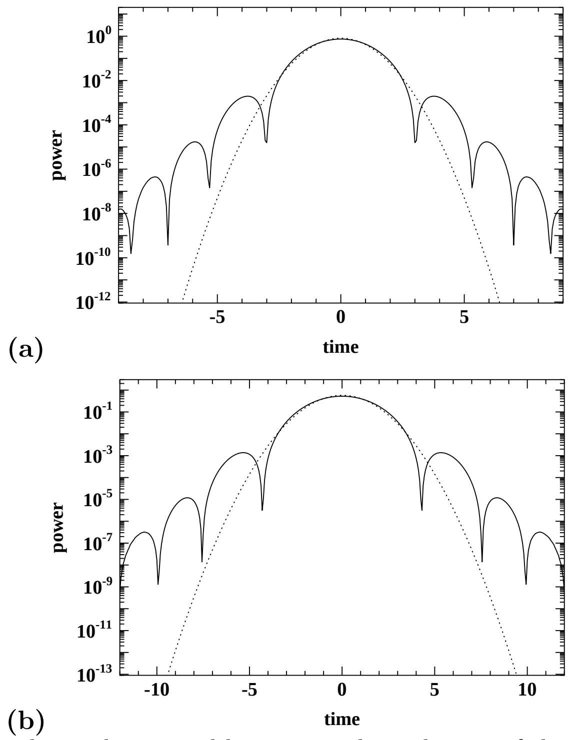

FIG. 5. Power profiles of the DM solitons determined by numerical simulations of the NLS equation (solid lines) compared with the theoretically predicted Gaussian pulses (dotted lines). Here $d_m = 0$, $C_E = 1$, $l_+ = l_- = 0.1$, $D_L = 10$ (a), and $D_L = 20$ (b).

Negative-mean dispersion. We have focused our attention to the stable stationary point. The comparisons between theory and numerical simulations are very similar to the zero-mean dispersion case (see Tables V-VI). The disagreement between the theoretical predictions and the numerical values of the rms widths are of the order of 9 %, because the DM soliton has a shape with heavy oscillatory tails that is now quite different from the Gaussian ansatz. It is however striking that a very small modification of the mean residual dispersion (from $\beta_{2\mathrm{mean}} = 0$ to $\beta_{2\mathrm{mean}} = 0.005$ ps^2/km) involves important changes of the pulse parameters. This is a first indication that the DM soliton is more sensitive to GVD fluctuations in this regime.

IV. RANDOM FLUCTUATIONS OF THE DISPERSION

Let us assume that $d_1(z) = d_m + m(z)$ where d_m is the mean residual dispersion and m is a zero-mean random process. The long-scale dynamics of the soliton parameters $(\bar{a}, \bar{b})$ is now driven by:

$$\frac{d\bar{a}}{dz} = f_a(\bar{a}, \bar{b}, d_m) + m_d(z)\bar{b}, \tag{14a}$$

$$\frac{d\bar{b}}{dz} = f_b(\bar{a}, \bar{b}, d_m) + 4m_d(z)\bar{a}^{-3}, \tag{14b}$$

where m_d is given by:

$$m_d(z) = \frac{1}{l_{\mathrm{map}}} \int_0^{l_{\mathrm{map}}} m([z/l_{\mathrm{map}}]l_{\mathrm{map}} + \zeta)d\zeta.$$

The complete and analytic study of this system is very intricate. Rather we shall focus on the stability of the point $(a_s, 0)$ which is stationary for the unperturbed problem (with $m \equiv 0$). Of course this point is no more stable when $m \not\equiv 0$. We shall assume that the random fluctuations are described by a white noise model. This is valid as soon as the correlation length of the process m is smaller than $2\pi/\sqrt{\gamma}$ which is always the case for practical applications. In such conditions we can prove by standard probability tools that the pair $(\bar{a}, \bar{b})$ is a diffusion Markov process whose probability density function satisfies the Fokker-Planck equation:

$$\frac{\partial p}{\partial z} = \mathcal{L}^* p, \qquad p(z=0,a,b) = \delta(a-a_s)\delta(b), \tag{15}$$

where $\mathcal{L}^*$ is the operator:

$$\begin{aligned} \mathcal{L}^* = & -\left(f_a(\bar{a},\bar{b},d_m) + \frac{2\sigma^2}{\bar{a}^3}\right)\frac{\partial}{\partial \bar{a}} \\ & -\left(f_b(\bar{a},\bar{b},d_m) - \frac{6\sigma^2\bar{b}}{\bar{a}^4}\right)\frac{\partial}{\partial \bar{b}} \\ & +\frac{\sigma^2\bar{b}^2}{2}\frac{\partial^2}{\partial \bar{a}^2} + \frac{4\sigma^2\bar{b}}{\bar{a}^3}\frac{\partial^2}{\partial \bar{a}\partial \bar{b}} + \frac{8\sigma^2}{\bar{a}^6}\frac{\partial^2}{\partial \bar{a}^2}. \end{aligned} \tag{16}$$

The parameter σ^2 is given by:

$$\begin{aligned} \sigma^2 &= 2\int_0^\infty \langle m_d(z) m_d(z+z')\rangle \, dz' \\ &= 2\int_0^\infty \langle m(z) m(z+z')\rangle \, dz'. \end{aligned}$$

where the brackets stand for the statistical averaging. Note that all moments of $\bar{a}$ can be deduced from the probability density function by a straightforward integration:

$$\langle \bar{a}(z)^n \rangle = \int da \int db \; a^n p(z,a,b) \tag{17}$$

Note also that in the limit $D_L \ll d_m^2/C_E^2$ the problem can be regarded as the random Kepler problem [27]. The pulse broadening and the eventual disintegration of the soliton in this averaged dynamics limit was addressed in [28]. The goal of the forthcoming section is precisely to analyze the case $D_L > d_m^2/C_E^2$ and to show that a strong dispersion management can succeed in stabilizing the soliton.

A. Stability of the stationary point

We would like now to discuss the dynamics of the processes $\bar{a}$ and $\bar{b}$ by first studying the linear stability of the stationary point $(a_s, 0)$ driven by the process m_d. The straightforward linearization of the system (14) around the point $(a_s, 0)$ leads to:

$$\frac{da_1}{dz} = \partial_b f_a b_1 + m_d(z) b_1, \tag{18a}$$

$$\frac{db_1}{dz} = \partial_a f_b a_1 + 4 m_d(z) a_s^{-3} - 12 m_d(z) a_s^{-4} a_1. \tag{18b}$$

The linearization (18) is valid in a deterministic framework, when $a_1^2 \ll a_1 \ll 1$. However we must pay attention that in a stochastic framework it may happen that $\langle a_1^2 \rangle \sim \langle a_1 \rangle \ll 1$, or even that $\langle a_1 \rangle \ll \langle a_1^2 \rangle \ll 1$ in case a_1 is a zero-mean process [29]. Accordingly it is necessary to expand system (14) at least to second order with respect to powers of the modulations a_1 and b_1:

$$\frac{da_1}{dz} = \partial_b f_a b_1 + \partial_{ab} f_a a_1 b_1 + m_d(z) b_1, \tag{19a}$$

$$\begin{aligned} \frac{db_1}{dz} = & \; \partial_a f_b a_1 + \frac{1}{2}\partial_a^2 f_b a_1^2 + \frac{1}{2}\partial_b^2 f_b b_1^2 + 4 m_d(z) a_s^{-3} \\ & -12 m_d(z) a_s^{-4} a_1 + 24 m_d(z) a_s^{-5} a_1^2. \end{aligned} \tag{19b}$$

The expressions of the second-order derivatives of the functions f_a and f_b can be found in Appendix B.

B. The system for the moments

We can write a closed-form system of ordinary differential equations for the first moments of the processes a_1 and b_1 by applying the Furutzu-Novikov formula [29], commonly called Itô's formula in the mathematical literature [30, p. 145]. Denoting

$$X = \begin{pmatrix} \langle a_1 \rangle \\ \langle b_1 \rangle \\ \langle a_1^2 \rangle \\ \langle b_1^2 \rangle \\ \langle a_1 b_1 \rangle \end{pmatrix},$$

$$M_0 = \begin{pmatrix} 0 & \partial_b f_a & 0 & 0 & \partial^2_{ab} f_a \\ \partial_a f_b & 0 & \frac{1}{2}\partial^2_{aa} f_b & \frac{1}{2}\partial^2_{bb} f_b & 0 \\ 0 & 0 & 0 & 0 & 2\partial_b f_a \\ 0 & 0 & 0 & 0 & 2\partial_a f_b \\ 0 & 0 & \partial_a f_b & \partial_b f_a & 0 \end{pmatrix},$$

$$M_1 = \begin{pmatrix} -6a_s^{-4} & 0 & 12a_s^{-5} & 0 & 0 \\ 0 & -6a_s^{-4} & 0 & 0 & 24a_s^{-5} \\ 4a_s^{-3} & 0 & -12a_s^{-4} & 1 & 0 \\ -96a_s^{-7} & 0 & 336a_s^{-8} & -12a_s^{-4} & 0 \\ 0 & 6a_s^{-3} & 0 & 0 & -24a_s^{-4} \end{pmatrix},$$

$$V = \begin{pmatrix} 2a_s^{-3} \\ 0 \\ 0 \\ 16a_s^{-6} \\ 0 \end{pmatrix},$$

the system that governs the evolutions of the first moments of the soliton width and chirp is:

$$\frac{dX}{dz} = M_0 X + \sigma^2 M_1 X + \sigma^2 V. \tag{20}$$

The term $\sigma^2 V$ is the source of the random instability. The term $\sigma^2 M_1 X$ is responsible for a stochastic resonance phenomenon. Indeed M_0 has only pure imaginary eigenvalues, but $M_0 + \sigma^2 M_1$ has a positive eigenvalue. Of course, the term $\sigma^2 M_1 X$ is in a first step much smaller than the two other terms of the right-hand side, but it will eventually involve an exponential growth of the moments of a_1. We shall first carry out a study of the system by neglecting the stochastic resonance.

C. Diffusive pulse broadening

In this section we neglect the stochastic resonance phenomenon so we substitute 0 for $\sigma^2 M_1 X$ in Eq. (20). The more detailed study where the this term is taken into account will be carried out in Sections IV E-IV G. The system of equations for the moments of the processes a_1 and b_1 is:

$$\frac{dX}{dz} = M_0 X + \sigma^2 V.$$

Note that we can solve the system for the three second-order moments, and then substitute the result in the equations for the first-order moments. Solving these systems establish the two following identities for the first two moments (mean and variance of the width increment):

$$\langle a_1^2 \rangle = 8\frac{\sigma^2 \partial_b f_a}{a_s^6 |\partial_a f_b|}\left(z - \frac{\sin(2\sqrt{\gamma}z)}{2\sqrt{\gamma}}\right), \tag{21a}$$

$$\langle a_1 \rangle = \frac{2\sigma^2}{3|\partial_a f_b| a_s^6}\left(6c_0 z + \frac{\sin(\sqrt{\gamma}z)}{\sqrt{\gamma}} f(z)\right), \tag{21b}$$

$$f(z) = c_1 - c_2 \cos(\sqrt{\gamma}z),$$

where

$$c_0 = -\partial^2_{aa} f_b \frac{\partial_b f_a}{\partial_a f_b} + \partial^2_{bb} f_b,$$

$$c_1 = 8\partial^2_{ab} f_a + 8\partial^2_{aa} f_b \frac{\partial_b f_a}{\partial_a f_b} - 4\partial^2_{bb} f_b - 3\partial_a f_b a_s^3,$$

$$c_2 = 8\partial^2_{ab} f_a + 2\partial^2_{aa} f_b \frac{\partial_b f_a}{\partial_a f_b} + 2\partial^2_{bb} f_b.$$

The moments of a_1 consist of two types of terms: periodic modulations with period $2\pi/\sqrt{\gamma}$ and a linear growth. After a few periods the linear growth prevails over the periodic modulations, so we can write that, if $\sqrt{\gamma}z > 1$, then the first moments of a_1 are:

$$\langle a_1 \rangle \simeq g_1 \sigma^2 z, \qquad g_1 = \frac{4}{a_s^6}\left(\frac{\partial^2_{aa} f_b \partial_b f_a}{|\partial_a f_b|^2} + \frac{\partial^2_{bb} f_b}{|\partial_a f_b|}\right),$$

$$\langle a_1^2 \rangle \simeq g_2 \sigma^2 z, \qquad g_2 = \frac{8\partial_b f_a}{a_s^6 |\partial_a f_b|}.$$

The growth rates g_1 and g_2 as a function of D_L are plotted in Figure 6.

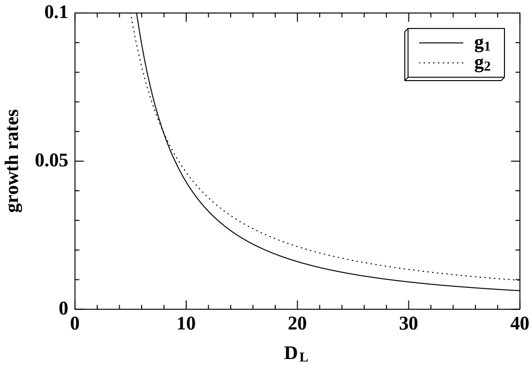

FIG. 6. Growth rates of the moments of the width increment versus DM strength. Here $d_m = 1$ and $C_E = 1$.

For strong DM we have:

$$\partial^2_{ab} f_a \simeq -C_E \frac{\alpha_s^2 (2 - 7\alpha_s^4 - 3\alpha_s^8)}{2(1+\alpha_s^4)^{5/2}} \simeq -0.162 C_E,$$

$$\partial^2_{aa} f_b \simeq \frac{C_E}{D_L^2} \frac{4(1 + 10\alpha_s^4 - 3\alpha_s^8)}{\alpha_s^2 (1+\alpha_s^4)^{5/2}} \simeq 20.12 \frac{C_E}{D_L^2},$$

and $\partial^2_{bb} f_b = -\partial^2_{ab} f_a$. In such conditions the first moments of a_1 are (for $\sqrt{\gamma}z > 1$):

$$\langle a_1 \rangle \simeq 4.66 D_L^{-3/2} \sigma^2 z, \tag{22a}$$

$$\langle a_1^2 \rangle^{1/2} \simeq 0.576 D_L^{-1/2} \sigma \sqrt{z}, \tag{22b}$$

while $a_s \simeq 0.549 D_L^{1/2}$. Accordingly, for a given amount of random fluctuations of the GVD coefficient, strong dispersion management tends to stabilize the pulse since both the first and second moments of the increment of the pulse width are reduced. Furthermore we can compare these results with the formulas that give the moments of the rms width of a Gaussian pulse in linear randomly dispersive medium (see Appendix C). For strong DM:

$$\langle T_{rms}(z) - T_{rms0} \rangle_{DMsoliton} \simeq 0.048 \frac{\sigma^2 z}{T_{rms0}^3}, \tag{23a}$$

$$\left\langle (T_{rms}(z) - T_{rms0})^2 \right\rangle_{DMsoliton}^{1/2} \simeq 0.079 \frac{\sigma \sqrt{z}}{T_{rms0}}, \tag{23b}$$

while in linear media:

$$\langle T_{rms}(z) - T_{rms0} \rangle_{linear} \simeq 0.125 \frac{\sigma^2 z}{T_{rms0}^3}, \tag{24a}$$

$$\left\langle (T_{rms}(z) - T_{rms0})^2 \right\rangle_{linear}^{1/2} \simeq 0.217 \frac{\sigma^2 z}{T_{rms0}^3}. \tag{24b}$$

The comparison of formulas (23a) and (24a) demonstrate that the mean increase rate of the rms width of a DM soliton is smaller than the corresponding rate for a linear pulse. If we focus our attention on the second moments, then we can deduce that dispersion fluctuations induce oscillations of the DM soliton width which are stronger than the mean increase in the early steps of propagation ($\sigma^2 z \ll T_{rms0}^4$). For longer propagation distances ($\sigma^2 z \sim T_{rms0}^4$), the mean increase will become of the same order as the width oscillations and the initial pulse width. These strong width oscillations are very different from the typical linear pulse broadening where the pulse rms width is always larger than the input width, and the mean and standard deviation of the rms width are of the same order.

The results can still be refined in the sense that the above analysis can be used to derive the statistical distribution of a_1. First of all we can actually compute the moments of all order. It is found in particular that, for any integer n:

$$\left\langle a_1^{2n} \right\rangle = \frac{(2n)!}{2^n n!} \left\langle a_1^2 \right\rangle^n . \tag{25}$$

Thus the moments of even order satisfy the combination rules of zero-mean Gaussian random variables. However the existence of small non-zero odd moments show that the statistical distribution of a_1 is close to that of a normal random variable, but with a slight asymmetry which strengthens the right tail of the probability density function of a_1 (which corresponds to an increment of the pulse width) while it diminishes the left tail of the probability density function (which corresponds to a decay of the pulse width). If we do not care of this asymmetry, we can claim that the probability distribution of $a_1(z)$ is Gaussian, hence the probability density function of T_{rms} is:

$$p(t) = \frac{\sqrt{2}}{\sqrt{\pi \langle a_1^2 \rangle}} \exp\left(-2 \frac{(t - T_{rms0})^2}{\langle a_1^2 \rangle} \right). \tag{26}$$

If we compare this result with the corresponding formula for the probability density function of the rms width of a pulse in randomly dispersive linear media (see Appendix C), then we find that the distribution tail decays faster for the DM soliton than for a linear pulse.

D. Numerical simulations

In this section we consider a dispersion map of one of two kinds presented in Table I. The DM solitons that have been derived in Section III D are launched in the middle of the first span. We also assume random fluctuations of the GVD coefficient. More exactly we consider a random process m which is stepwise constant over elementary intervals with length $\delta z = 0.1$ and take values m_j over the j-th interval. The m_j's are assumed to be independent random variables whose statistical distribution is uniform between -1 and 1. Accordingly the parameter σ^2 is equal to 0.033. The numerical solutions of the random NLS equation are found by using the split step Fourier method. For each simulation we record the rms pulse width $T_{rms}(z)$ at the middle of the first span of every map. In Figures 7 we plot the normalized first, second, and fourth moments of the pulse broadenings defined by:

$$DT_j = \left\langle (T_{rms}(z) - T_{rms0})^j \right\rangle^{1/j}, \quad j = 1, 2, 4. \tag{27}$$

The numerical values are averaged over 10^4 realizations. They are compared with the theoretical formulas $\left\langle a_1^j \right\rangle^{1/j} /2$ given by Eqs. (21a-21b-25) (remember that $T_{rms}(z) - T_{rms0} = a_1/2$ in the theoretical Gaussian framework). The close agreements demonstrate that our approach is efficient for predicting the behaviors of solitons in random media.

Agreement is also found when comparing the theoretical probability density functions of the pulse rms widths with the numerical histograms (Figure 8).

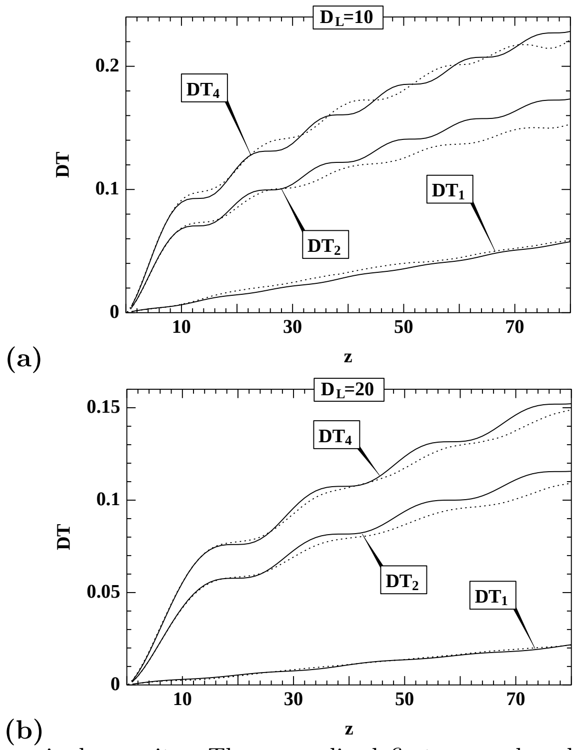

FIG. 7. Pulse broadening in dimensionless units. The normalized first, second and fourth moments of the pulse width increments are plotted. The solid lines stand for the theoretical values, the dotted lines represent the numerical values averaged over 10^4 realizations.

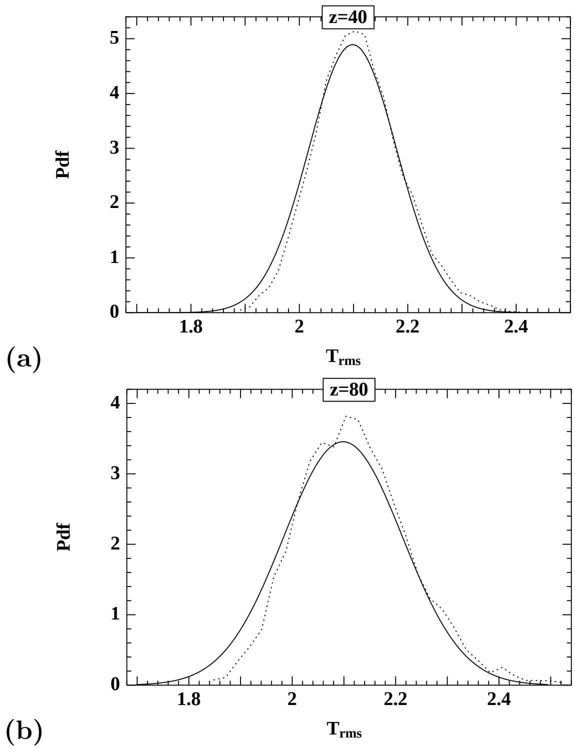

FIG. 8. Probability density functions of the pulse rms widths. for the configuration B ($D_L = 20$). The solid lines stand for the theoretical functions given by Eq. (26), the dotted lines represent the numerical histograms computed from 10^4 realizations.

E. Stochastic resonance

The next step in the study of the stability with respect to random dispersive fluctuations is to check that a possible stochastic resonance phenomenon cannot involve a dramatic instability growth. Indeed the analysis in Section III has exhibited periodic oscillations of the soliton dynamics with the period $2\pi/\sqrt{\gamma}$. In the case where the soliton propagates over distances larger than $2\pi/\sqrt{\gamma}$, we should carefully take into account the stochastic resonance phenomenon. For this we study the system (19). This system is of the type parametric resonance with a source term. Note that the source term $4\sigma m_d(z)a_s^{-3}$ is all the smaller as the dispersion management is stronger, because a_s is an increasing function of D_L. However this remark is not sufficient to conclude to the efficiency of the dispersion management to the stabilization of the DM soliton, since it is well-known in stochastic parametric resonance that the exponential gain of the homogeneous system (without the source term) is the main parameter that controls the stability of the system.

We now compute the Lyapunov exponent of the homogeneous system:

$$\frac{da_2}{dz} = (\partial_b f_a + \sigma m_d(z))b_2,$$
$$\frac{db_2}{dz} = (\partial_a f_b - 12a_s^{-4}\sigma m_d(z))a_2.$$

Setting:

$$a_2 = R\sqrt{\partial_b f_a}\cos(\psi),$$
$$b_2 = R\sqrt{-\partial_a f_b}\sin(\psi),$$

this system also reads:

$$R(z) = R_0 \exp\left(\sigma \int_0^z q(m_d(s), \psi(s))ds\right), \tag{28a}$$

$$\frac{d\psi}{dz} = -\sqrt{\gamma} + \sigma h(m_d(z), \psi(z)), \tag{28b}$$

where

$$\begin{aligned} q(m,\psi) &= -g_c m \sin(2\psi), \\ h(m,\psi) &= m\left(\frac{12a_s^{-4}\partial_b f_a - \partial_a f_b}{2\sqrt{\gamma}} - g_c\cos(2\psi)\right), \\ g_c &:= \frac{12a_s^{-4}\partial_b f_a + \partial_a f_b}{2\sqrt{\gamma}}. \end{aligned} \tag{29}$$

We can compute by standard probability theory the Lyapunov exponent that governs the growth of (a_2, b_2):

$$G := \lim_{z\to\infty} \frac{1}{z}\ln R(z). \tag{30}$$

In case of a white noise m_d it is found that [31]:

$$G = \frac{\sigma^2 g_c^2}{2}, \tag{31}$$

where g_c is given by (29).

In the case $d_m > 0$ the exponent g_c^2 is of the form:

$$g_c^2 = \frac{C_E^4}{d_m^4} G_c^2\left(D_L\frac{C_E^2}{d_m^2}\right), \tag{32}$$

where $D \mapsto G_c(D)$ is dimensionless. Thus we can expand the exponent g_c^2 as powers of $D_L C_E^2/d_m^2$:

$$g_c^2 \overset{D_L \ll d_m^2/C_E^2}{\simeq} \frac{C_E^4}{4d_m^4}\left(1 - D_L^2 \frac{C_E^4}{d_m^4}\frac{17}{24} + O(D_L^4 \frac{C_E^8}{d_m^8})\right), \tag{33}$$

while for very strong DM (cf. Remark 1) we have:

$$g_c^2 \overset{D_L \gg d_m^2/C_E^2}{\simeq} \frac{(5\alpha_s^4 - 2)^2}{2(1-\alpha_s^4)\alpha_s^8} D_L^{-2} \simeq 159.7 D_L^{-2}. \tag{34}$$

We can also plot the exponent g_c^2 as a function of D_L (see Figure 9). This puts into evidence that the larger the dispersion management, the smaller the Lyapunov exponent. Although the decay is not monotonous, the general picture is that the instability gain is reduced as the dispersion management is strong. More striking: there exists one value of the DM strength for which the exponent g_c^2 vanishes, which is around $D_L = 6.25 d_m^2 C_E^{-2}$. At this point the Lyapunov exponent is zero. This particular point is accessible in the real world, as D_L is typically of the order of 10 (see Tables I-IV), and the condition $d_m \simeq C_E$ simply means that the mean residual dispersion effect has a comparable magnitude as the nonlinear effect. In the physical variables the condition $D_L = 6.25 d_m^2 C_E^{-2}$ reads exactly as

$$\sqrt{D_+ L_+ - D_- L_-} = 0.4 \frac{\lambda^2 A_{\rm eff} D_{\rm mean}}{\sqrt{c} n_2 \mathcal{E}_{pulse}}.$$

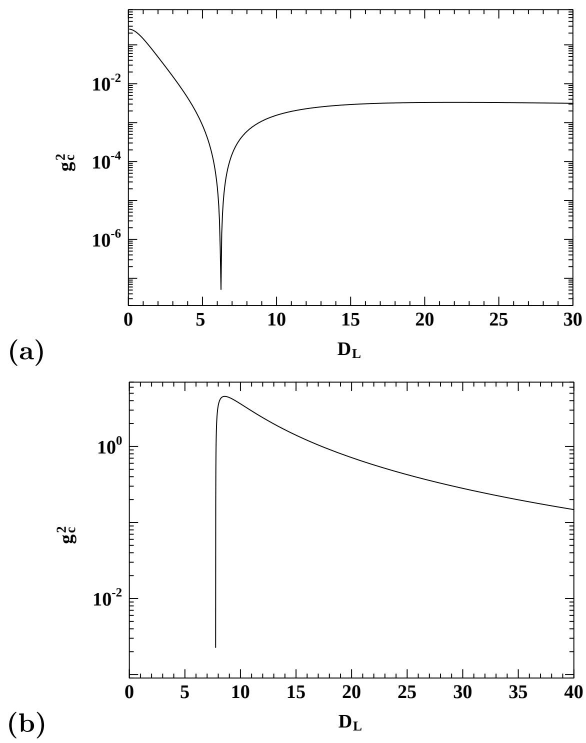

FIG. 9. Instability gain g_c^2 of the stationary point as a function of the dispersion strength D_L for $C_E = 1$, $d_m = 1$ (picture a), and $d_m = -0.05$ (picture b).

In the case $d_m < 0$ the scaling identity (32) still holds true. Plotting the gain g_c^2 for a reasonable set of parameters d_m and C_E shows that the Lyapunov exponent may reach large values for a weak DM, so that the DM soliton would be unstable with respect to random dispersive fluctuations in this regime. For very strong DM we get back the behavior (34).

In the limit configuration $d_m = 0$ the Lyapunov exponent is:

$$g_c^2 = \frac{(5\alpha_s^4 - 2)^2}{2\alpha_s^8(1-\alpha_s^4)} D_L^{-2} \simeq 159.7 D_L^{-2}.$$

F. Evolution of the soliton width

The system that governs the evolutions of the first moments of the soliton width and chirp is Eq. (20). The solution of the system is:

$$X(z) = \sigma^2 \int_0^z \exp\left((M_0 + \sigma^2 M_1)s\right) ds V. \tag{35}$$

The closed-form expressions of the moments of a_1 are too complicated to be written here. However we can plot the result by straightforward numerical integration.

The stochastic resonance phenomenon is related to the parameter g_c^2. If $\sigma^2 g_c^2 z \ll 1$, then the stochastic resonance cannot grow and the term $\sigma^2 M_1$ can be neglected in the system for the moments. This gives a criterion for the validity of the analysis performed in Section IV C. If $\sigma^2 g_c^2 z$ reaches values of order 1, then stochastic resonance cannot be neglected. It should be noted that, as soon as the exponential growth appears, the pulse width will reach high values which makes the expansion of system (14) into system (19) not valid anymore. Thus, in case of stochastic resonance, the complete system (14) should be addressed and one should consider the complete Fokker-Planck equation (15).

Considering the practical applications and typical fiber parameters such as those presented in Tables I-IV, stochastic resonance can appear only when $d_m < 0$ or $0 \leq d_m \ll C_E$. In these conditions we also have $g_c^2 \simeq 160 D_L^{-2}$, so that stochastic resonance will arise if $160 D_L^{-2} \sigma^2 z \geq 1$. Remember that $\sigma^2 z$ is the mean square cumulative random dispersion in dimensionless units. In the physical variables the condition $d_m < 0$ or $0 \leq d_m \ll C_E$ reads $D_{\rm mean} < 0$ or $0 \leq \frac{\lambda^3 A_{\rm eff} D_{\rm mean}}{4\pi^{3/2} c T_{pulse} n_2 \mathcal{E}_{pulse}} \ll 1$ (equivalently the scale corresponding to the residual dispersion is much larger than the nonlinear length scale). The condition $160 D_L^{-2} \sigma^2 z \geq 1$ reads $\left\langle \left(\int_0^Z D_{rand}(S) dS \right)^2 \right\rangle \geq (D_+ L_+ - D_- L_-)^2 / 640$, where L_+, L_-, and Z are expressed in km, while D_+, D_-, and D_{rand} (the random component of the distance-varying dispersion parameter) are expressed in ps/nm/km.

G. New numerical simulations

The stochastic resonance phenomenon is negligible in the conditions of our first numerical simulations in Section IV D. Indeed, the positive mean dispersion makes the parameter g_c^2 very small (see Figure 9). However, if the mean dispersion is zero, then the value of the parameter $g_c^2 \simeq 160 D_L^{-2}$ shows that the stochastic resonance phenomenon should be taken into account. In this section we consider a dispersion map of one of three kinds described in Tables III-IV. We consider random fluctuations of the GVD coefficient with $\sigma^2 = 0.033$. We perform the same job as in Section IV D. The only but important difference is that the theoretical values are computed from the resolution of the moment equations obtained from the Fokker-Planck equation (15). The results are plotted in Figure 10. The stochastic resonance obviously plays a primary role for $D_L = 10$, since the simplified Eq. (21b) predicts a mean square pulse broadening $DT_2 \simeq 0.15$ for $z = 80$, while it is actually around 0.4.

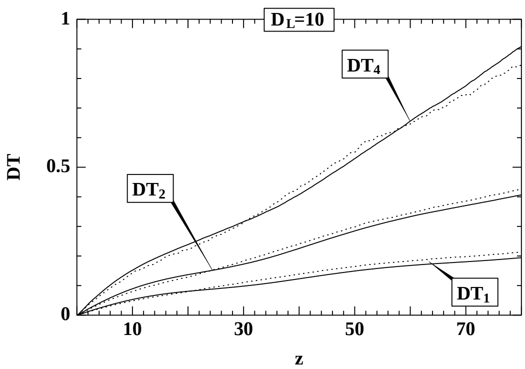

(a)

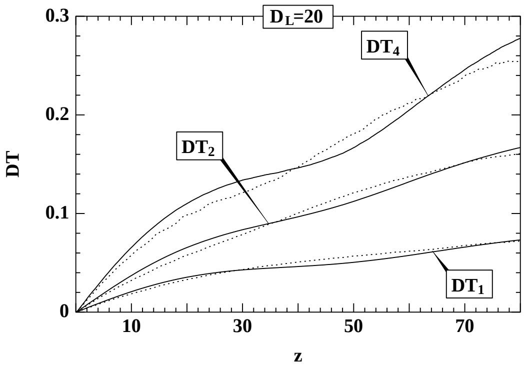

(b)

FIG. 10. Pulse broadening in dimensionless units. The normalized first, second and fourth moments of the pulse width increments as defined by Eq. (27) are plotted. The solid lines stand for the theoretical values, the dotted lines represent the numerical values averaged over 10^4 realizations.

V. CONCLUSION

A theoretical investigation of the stability of DM solitons is proposed that is based on a technique of separation of scales. It provides a fast and efficient way to compute all relevant quantities. We give precise asymptotic expressions for the widths and chirps of the stable solitons, as well as conditions for their stabilities in homogeneous and inhomogeneous media.

The solitons corresponding to strong dispersion managements are more stable with respect to the influence of random fluctuations of the chromatic dispersion than the solitons corresponding to weak dispersion managements. A stochastic resonance phenomenon may induce a dramatic pulse broadening in the normal or zero-mean dispersion regimes. However a small amount of positive residual dispersion is sufficient to prevent from this exponential growth. A particular value of the residual dispersion can even succeed in canceling the Lyapunov exponent of the stochastic resonance, but it does not prevent from a diffusive growth.

We could wonder whether the approach proposed in this paper can be generalized to any type of random perturbations of the DM soliton propagation. It should be noted that random dispersive fluctuations are compatible with the Gaussian ansatz of the pulse shape, since a chirped Gaussian pulse is the self-similar form for the linear randomly dispersive regime. That is why it is not surprising that our results are so good. If a different type of perturbation is addressed, as for instance polarization mode dispersion [32,33], that does not preserve the Gaussian shape, then a more elaborate ansatz should be used [34]. If a perturbation is considered that involves strong radiative effects, then the ansatz approach is not valid anymore. However it should be possible to apply a separation of scales technique and derive an averaged variational principle on the partial differential equation itself. This approach has been proposed recently [35], and we do believe that it could be useful for the next step of the study of the stabilizing effects of dispersion management.

ACKNOWLEDGMENTS

We thank S. Wabnitz for useful and stimulating discussions.

REFERENCES

[1] M. Suzuki, I. Morita, N. Edagawa, S. Yamamoto, H. Taga, and S. Akiba, Electron. Lett. **31** (1995) 2027.
[2] N. Smith, F. M. Knox, N. J. Doran, K. J. Blow, and I. Bennion, Electron. Lett. **32** (1996) 54.
[3] I. Gabitov and S. K.Turitsyn, Opt. Lett. **21** (1996) 327; JETP Lett. **63** (1996) 862.
[4] W. Forysiak, F. M. Knox, and N. J. Doran, J. Lightwave Technol. **12** (1994) 1330.
[5] W. Forysiak, K. J. Blow, and N. J. Doran, Electron. Lett. **29** (1993) 1225.
[6] N. J. Doran, N. J. Smith, W. Forysiak, and F. M. Knox, in *Physics and applications of optical solitons in fibers '95* (Kluwer, 1996) 1.
[7] A. Hasegawa, S. Kumar, and Y. Kodama, Opt. Lett. **21** (1996) 39.
[8] A. Hasegawa and F. Tappert, Appl. Phys. Lett. **23** (1973) 142.
[9] P. V. Mamyshev and L. F. Mollenauer, Optics Lett. **21** (1996) 396.

[10] C. Lin, H. Kogelnik, and L. G. Cohen, Optics Lett. **5** (180) 476.
[11] S. K. Turitsyn, T. Schäfer, K. H. Spatschek, and V. K. Mezentzev, Opt. Commun. **163** (1999) 122.
[12] Y. Kodama, A. Maruta, and A. Hasegawa, Quantum Opt. **6** (1994) 463.
[13] S. Wabnitz, Y. Kodama, and A. B. Aceves, Opt. Fiber Techn. **1** (1995) 187.
[14] L. F. Mollenauer, P. V. Mamyshev, and M. J. Neubelt, Opt. Lett. **21** (1996) 1724.
[15] J. Grip and L. F. Mollenauer, Opt. Lett. **23** (1998) 1603.
[16] F. Kh. Abdullaev, S. A. Darmanyan, A. Kobyakov, and F. Lederer, Phys. Lett. A **220** (1996) 213.
[17] G. P. Agrawal, Nonlinear fiber optics, 2nd ed., Academic Press, New York, 1995.
[18] A. Hasegawa and Y. Kodama, Opt. Lett. **15** (1990) 1444.
[19] K. J. Blow and N. J. Doran, IEEE Photon. Technol. Lett. **3** (1991) 369.
[20] S. K. Turitsyn, JETP Lett. **65** (1997) 845.
[21] S. K. Turitsyn, A. B. Aceves, C. K. R. T. Jones, and V. Zharnitsky, Phys. Rev. E **58** (1998) 1.
[22] D. Anderson, Phys. Rev. A **27** (1983) 1393.
[23] S. K. Turitsyn, I. Gabitov, E. W. Laedke, V. K. Mezentsev, S. L. Musher, E. G. Shapiro, T. Schäfer, and K. H. Spatschek, Opt. Commun. **151** (1998) 117.
[24] B. A. Malomed, D. F. Parker, and N. F Smyth, Phys. Rev. E **48** (1993) 1418.
[25] Y. Kodama, in *New trends in optical soliton transmission systems* (Kluwer, 1998) 131.
[26] J. H. B. Nijhof, N. J. Doran, W. Forysiak, and F. M. Knox, Electron. Lett. **33** (1997) 1726.
[27] F. Kh. Abdullaev, J. Bronski, and G. Papanicoalou, Physica D **135** (1999) 369.
[28] F. Kh. Abdullaev and B. B. Baizakov, Opt. Lett. **25** (2000) 93.
[29] V. I. Klyatskin, Stochastic differential equations and waves in random media, Nauka, Moscow, 1980.
[30] D. Revuz and M. Yor, Continuous martingales and Brownian motion, Springer, Berlin, 1991.
[31] L. Arnold, G. Papanicolaou, and V. Wihstutz, SIAM J. Appl. Math. **46** (1986) 427.
[32] C. R. Menyuk, J. Opt. Soc. Am. B **5** (1988) 392.
[33] S. G. Evangelides, L. F. Mollenauer, J. P. Gordon, and N. S. Bergano, J. Lightwave Technol. **10** (1992) 28.
[34] F. Kh. Abdullaev, B. A. Umarov, M. R. B. Wahiddin, and D. V. Navotny, J. Opt. Soc. Am. B **17** (2000) 1117.
[35] V. Zharnitsky, E. Grenier, C. K. R. T. Jones, and S. K. Turitsyn, Physica D **152** (2001) 794.
[36] N. M. Krylov and N. N. Bogoliubov, Introduction to nonlinear mechanics, Princeton University Press, Princeton, 1957.
[37] L. F. Mollenauer, P. V. Mamyshev, J. Gripp, M. J. Neubelt, N. Mamysheva, L. Grner-Nielsen, and T. Veng, Opt. Lett. **25** (2000) 704.

APPENDIX A: DERIVATION OF THE EFFECTIVE SYSTEM

To derive the effective system that governs the long-scale behavior of the soliton parameters we introduce a dimensionless parameter ε so that the dispersion maps reads $d_0(z) = \frac{1}{\varepsilon}\bar{d}_0(\frac{z}{\varepsilon})$. This means that we assume that the dispersion strength $D_L = d_+ l_+ = -d_- l_-$ is of order 1, and that the fiber span lengths l_+, l_- are smaller (of order ε) than all the other characteristic lengths of the problem. The process X^ε is solution of:

$$\frac{dX^\varepsilon}{dz} = \frac{1}{\varepsilon}\bar{d}_0(\frac{z}{\varepsilon})F(X^\varepsilon(z)) + G(X^\varepsilon(z), \frac{z}{\varepsilon}).$$

We denote by $\mathcal{X}$ the orbits:

$$\frac{d\mathcal{X}}{d\zeta}(X,\zeta) = \bar{d}_0(\zeta)F(\mathcal{X}), \quad \mathcal{X}(X,0) = X.$$

We assume that $\zeta \mapsto \mathcal{X}(X,\zeta)$ is periodic with respect to ζ for every X. It is easy to check that the map $X \mapsto \mathcal{X}(X,\zeta)$ is invertible for any ζ. We can write:

$$\mathcal{X}^{-1}\left(\mathcal{X}(X,\zeta),\zeta\right) = X. \tag{A1}$$

Accordingly, differentiating (A1) with respect to X yields:

$$\frac{\partial \mathcal{X}^{-1}(\mathcal{X},\zeta)}{\partial X} |_{\mathcal{X}=\mathcal{X}(X,\zeta)} = M^{-1}(X,\zeta), \tag{A2}$$

where M is the matrix given by $M(X,\zeta) = \frac{\partial \mathcal{X}}{\partial X}(X,\zeta)$. On the other hand, differentiating (A1) with respect to ζ establishes:

$$\frac{\partial \mathcal{X}^{-1}(\mathcal{X},\zeta)}{\partial \zeta} |_{\mathcal{X}=\mathcal{X}(X,\zeta)} = -\bar{d}_0(\zeta)M^{-1}(X,\zeta)F(\mathcal{X}(X,\zeta)). \tag{A3}$$

We then introduce:

$$\tilde{X}^\varepsilon(z) = \mathcal{X}^{-1}\left(X^\varepsilon(z), \frac{z}{\varepsilon}\right)$$

which obeys the ODE:

$$\frac{d\tilde{X}^\varepsilon(z)}{dz} = \frac{\partial \mathcal{X}^{-1}}{\partial X}(X^\varepsilon(z), \frac{z}{\varepsilon})\frac{dX^\varepsilon(z)}{dz} + \frac{1}{\varepsilon}\frac{\partial \mathcal{X}^{-1}}{\partial \zeta}(X^\varepsilon(z), \frac{z}{\varepsilon}).$$

Substituting Eqs. (A2-A3) into this ODE and taking into account the relation $X^\varepsilon(z) = \mathcal{X}\left(\tilde{X}^\varepsilon(z), \frac{z}{\varepsilon}\right)$ we get:

$$\frac{d\tilde{X}^\varepsilon(z)}{dz} = M^{-1}(\tilde{X}^\varepsilon(z), \frac{z}{\varepsilon})G(\mathcal{X}(\tilde{X}^\varepsilon(z), \frac{z}{\varepsilon}), \frac{z}{\varepsilon}).$$

The terms of order $O(1/\varepsilon)$ have disappeared, thus we can now average over the fast oscillations by standard homogenization techniques. We may for instance invoke the Bogolubov-Krylov averaging theorem [36] which yields that $\tilde{X}^\varepsilon(z)$ converges as $\varepsilon \to 0$ in the space of the continuous functions to $\bar{X}(z)$ solution of:

$$\frac{d\bar{X}(z)}{dz} = \bar{G}(\bar{X}(z), z), \qquad \bar{G}(X,z) := \frac{1}{l_{\rm map}}\int_0^{l_{\rm map}} d\zeta M^{-1}(\bar{X},\zeta)G(\mathcal{X}(X,\zeta), z+\zeta).$$

APPENDIX B: EXPLICIT EXPRESSIONS

The inverse of the matrix $M(a,b,s)$ is equal to:

$$M^{-1}(a,b,s) = \begin{pmatrix} \dfrac{a\left(a^2(a+bD_0(s))^3 + 4bD_0(s)^3\right)}{\left[a^2(a+bD_0(s))^2 + 4D_0(s)^2\right]^{3/2}} & \dfrac{-aD_0(s)(a+bD_0(s))}{\left[a^2(a+bD_0(s))^2 + 4D_0(s)^2\right]^{1/2}} \\ \dfrac{4D_0(s)\left(3a^3(a+bD_0(s)) + a^2b^2D_0(s)^2 + 4D_0(s)^2\right)}{a^2\left[a^2(a+bD_0(s))^2 + 4D_0(s)^2\right]^{3/2}} & \dfrac{a^3(a+bD_0(s)) - 4D_0(s)^2}{a^2\left[a^2(a+bD_0(s))^2 + 4D_0(s)^2\right]^{1/2}} \end{pmatrix}.$$

The exact expressions of f_a and f_b are:

$$
\begin{aligned}
f_a(a,b,d_m) &= d_m b + \frac{4C_E a^3}{D_L(4+a^2b^2)}\left(\frac{a-bD_L}{\sqrt{(2a-bD_L)^2a^2+4D_L^2}} - \frac{a+bD_L}{\sqrt{(2a+bD_L)^2a^2+4D_L^2}}\right)\\
&\quad + \frac{2C_E a^3 b}{D_L(4+a^2b^2)^{3/2}} \ln\left(\frac{2a^3b+\sqrt{4+a^2b^2}\sqrt{(2a+bD_L)^2a^2+4D_L^2}+D_L(4+a^2b^2)}{2a^3b+\sqrt{4+a^2b^2}\sqrt{(2a-bD_L)^2a^2+4D_L^2}-D_L(4+a^2b^2)}\right),\\
f_b(a,b,d_m) &= \frac{4d_m}{a^3} + \frac{4C_E}{D_L(4+a^2b^2)}\left(\frac{ba^3-4D_L}{\sqrt{(2a+bD_L)^2a^2+4D_L^2}} - \frac{ba^3+4D_L}{\sqrt{(2a-bD_L)^2a^2+4D_L^2}}\right)\\
&\quad + \frac{8C_E}{D_L(4+a^2b^2)^{3/2}} \ln\left(\frac{2a^3b+\sqrt{4+a^2b^2}\sqrt{(2a+bD_L)^2a^2+4D_L^2}+D_L(4+a^2b^2)}{2a^3b+\sqrt{4+a^2b^2}\sqrt{(2a-bD_L)^2a^2+4D_L^2}-D_L(4+a^2b^2)}\right).
\end{aligned}
$$

The expressions of f_a and f_b over the set $b=0$ are:

$$
\begin{aligned}
&f_a(a,b=0,d_m) = 0,\\
&f_b(a,b=0,d_m) = \frac{C_E a^3(D_L^2+a^4)\ln\left(\frac{\sqrt{D_L^2+a^4}+D_L}{\sqrt{D_L^2+a^4}-D_L}\right) + 4d_m D_L(D_L^2+a^4) - 4C_E a^3 D_L\sqrt{D_L^2+a^4}}{D_L a^3(D_L^2+a^4)}.
\end{aligned}
$$

At the point a_s where $f_b(a,0,d_m)=0$ the first derivatives of the functions f_a and f_b are:

$$
\begin{aligned}
&\frac{\partial f_a}{\partial a}(a_s,0,d_m) = 0,\\
&\frac{\partial f_a}{\partial b}(a_s,0,d_m) = \frac{C_E a_s^7}{2(D_L^2+a_s^4)^{3/2}},\\
&\frac{\partial f_b}{\partial a}(a_s,0,d_m) = 4\frac{C_E a_s^3(a_s^4-D_L^2) - 3d_m(D_L^2+a_s^4)^{3/2}}{a_s^4(D_L^2+a_s^4)^{3/2}},\\
&\frac{\partial f_b}{\partial b}(a_s,0,d_m) = 0,\\
&\frac{\partial^2 f_a}{\partial a^2}(a_s,0,d_m) = 0,\\
&\frac{\partial^2 f_a}{\partial a\partial b}(a_s,0,d_m) = -\frac{1}{2a_s}\left(\frac{C_E a_s^3(2D_L^4-7D_L^2a_s^4-3a_s^8)}{(D_L^2+a_s^4)^{5/2}} + 6d_m\right),\\
&\frac{\partial^2 f_a}{\partial b^2}(a_s,0,d_m) = 0,\\
&\frac{\partial^2 f_b}{\partial a^2}(a_s,0,d_m) = \frac{4}{a_s^5}\left(\frac{C_E a_s^3(D_L^4+10D_L^2a_s^4-3a_s^8)}{(D_L^2+a_s^4)^{5/2}} + 12d_m\right),\\
&\frac{\partial^2 f_b}{\partial a\partial b}(a_s,0,d_m) = 0,\\
&\frac{\partial^2 f_b}{\partial b^2}(a_s,0,d_m) = \frac{1}{2a_s}\left(\frac{C_E a_s^3(2D_L^4-7D_L^2a_s^4-3a_s^8)}{(D_L^2+a_s^4)^{5/2}} + 6d_m\right).
\end{aligned}
$$

APPENDIX C: PULSE BROADENING IN LINEAR RANDOMLY DISPERSIVE MEDIA

The pulse propagation in linear media is governed by the Schrödinger equation:

$$iu_z + \frac{d(z)}{2}u_{tt} = 0.$$

It is easy to solve analytically this equation when the input wave has Gaussian shape:

$$u(z=0,t) = \exp\left(-\frac{t^2}{a_0^2}\right).$$

We get that the wave keeps its Gaussian shape with distance-varying width and chirp:

$$u(z,t) = \frac{1}{a(z)} \exp\left(-\frac{t^2}{a(z)^2} + i\phi(z) + ic(z)t^2\right),$$

where

$$a(z) = a_0\sqrt{1+\frac{4D(z)^2}{a_0^4}}, \quad c(z) = \frac{2D(z)}{a_0^4+4D(z)^2} \quad \phi(z) = -\frac{1}{2}\arctan\left(\frac{2D(z)}{a_0}\right), \quad D(z) = \int_0^z d(s)ds.$$

Since the rms width is equal to $a/2$ in case of a Gaussian pulse we have:

$$T_{rms}(z) = T_{rms0}\left(1+\frac{D(z)^2}{4T_{rms0}^4}\right)^{1/2}. \tag{C1}$$

For any initial pulse u_0 the linear Schrödinger equation can be solved analytically in Fourier domain, so that the identity (C1) can be generalized to:

$$T_{rms}(z) = T_{rms0}\left(1+R_0 D(z)^2\right)^{1/2}, \text{ where } R_0 = \frac{\int |u_{0t}|^2 dt}{\int t^2 |u_0|^2 dt}.$$

This closed-form formula shows that the pulse width can only increase whatever its initial profile. If the GVD coefficient is a white noise with variance σ, then $D(z)$ obeys a normal distribution with zero mean and variance $\sigma^2 z$ and the statistical distribution of the pulse broadening can be readily estimated. Writing $T_{rms}(z) = T_{rms0} + T_1(z)$, the moments of the pulse width increment can be expanded as powers of $\sigma^2 z/T_{rms0}^3$ as:

$$\langle T_1^n \rangle^{1/n} = c_n \frac{\sigma^2 z}{8T_{rms0}^3} + O\left(\frac{\sigma^4 z^2}{T_{rms0}^6}\right), \qquad c_n = \left(\frac{(2n)!}{2^n n!}\right)^{1/n}.$$

The probability distribution of T_{rms} can be described in terms of a $\Gamma(1/2)$ random variable. More exactly the probability density function of T_{rms} is:

$$p(t) = \frac{1}{\sqrt{2\pi \langle T_1 \rangle (t-T_{rms0})}} \exp\left(-\frac{t-T_{rms0}}{2\langle T_1\rangle}\right) \mathbf{1}_{t\geq T_{rms0}}.$$

TABLE I. Dispersion maps and soliton parameters in physical units. P_{max} stands for the power peak. We assume $A_{\text{eff}} = 60$ μm^2, $n_2 = 3\ 10^{-2}$ nm^2/W, $\lambda_0 = 1.55$ μm, and $\mathcal{E}_{\text{pulse}} = 17.7$ fJ. In these conditions the mean dispersion is $\beta_{2\text{mean}} = -0.1$ ps^2/km.

	L_+	L_-	β_{2+}	β_{2-}	$T_{rms\text{DM}}$	$T_{rms\text{theo}}$	$P_{max\text{DM}}$	$P_{max\text{theo}}$
A	25 km	25 km	9.9 ps^2/km	-10.1ps^2/km	8.391 ps	8.396 ps	0.8434 mW	0.8422 mW
B	25 km	25 km	19.9 ps^2/km	-20.1 ps^2/km	10.491 ps	10.576 ps	0.6608 mW	0.6686 mW

TABLE II. Dispersion map and soliton parameters in dimensionless units. The typical power is $P_0 = 2$ mW, the typical nonlinear length is $Z_0 = 250$ km, and the typical time is $T_0 = 5$ ps.

	l_+	l_-	d_+	d_-	d_m	C_E	$T_{rms\text{DM}}$	$T_{rms\text{theo}}$	$\max(\lvert u\rvert^2)_{\text{DM}}$	$\max(\lvert u\rvert^2)_{\text{theo}}$
A	0.1	0.1	100	-100	1	1	1.6782	1.6793	0.4217	0.4211
B	0.1	0.1	200	-200	1	1	2.0983	2.1152	0.3304	0.3343

TABLE III. Dispersion maps and soliton parameters in physical units. We also assume $A_{\text{eff}} = 60\ \mu\text{m}^2$, $n_2 = 3\ 10^{-2}\ \text{nm}^2/\text{W}$, $\lambda_0 = 1.55\ \mu\text{m}$, and $\mathcal{E}_{\text{pulse}} = 17.7$ fJ. In these conditions the mean dispersion is $\beta_{2_{\text{mean}}} = 0\ \text{ps}^2/\text{km}$.

	L_+	L_-	β_{2_+}	β_{2_-}	$T_{rms\text{DM}}$	$T_{rms\text{theo}}$	$P_{max\text{DM}}$	$P_{max\text{theo}}$
C	25 km	25 km	10 ps^2/km	-10 ps^2/km	4.624 ps	4.338 ps	1.4394 mW	1.6299 mW
D	25 km	25 km	20 ps^2/km	-20 ps^2/km	6.545 ps	6.136 ps	1.0490 mW	1.1524 mW

TABLE IV. Dispersion maps and DM soliton parameters in dimensionless units. The typical power is $P_0 = 2$ mW, the typical nonlinear length is $Z_0 = 250$ km, and the typical time is $T_0 = 5$ ps.

	l_+	l_-	d_+	d_-	d_m	C_E	$T_{rms\text{DM}}$	$T_{rms\text{theo}}$	$\max(\|u\|^2)_{\text{DM}}$	$\max(\|u\|^2)_{\text{theo}}$
C	0.1	0.1	100	-100	0	1	0.9248	0.8677	0.7430	0.8149
D	0.1	0.1	200	-200	0	1	1.3090	1.2272	0.5245	0.5762

TABLE V. Dispersion maps and soliton parameters in physical units. We also assume $A_{\text{eff}} = 60\ \mu\text{m}^2$, $n_2 = 3\ 10^{-2}\ \text{nm}^2/\text{W}$, $\lambda_0 = 1.55\ \mu\text{m}$, and $\mathcal{E}_{\text{pulse}} = 17.7$ fJ. In these conditions the mean dispersion is $\beta_{2_{\text{mean}}} = 0.005\ \text{ps}^2/\text{km}$.

	L_+	L_-	β_{2_+}	β_{2_-}	$T_{rms\text{DM}}$	$T_{rms\text{theo}}$	$P_{max\text{DM}}$	$P_{max\text{theo}}$
E	25 km	25 km	10.005 ps^2/km	-9.995 ps^2/km	3.8555 ps	3.5250 ps	1.7586 mW	2.0060 mW
F	25 km	25 km	20.005 ps^2/km	-19.995 ps^2/km	5.9260 ps	5.4745 ps	1.1542 mW	1.2916 mW

TABLE VI. Dispersion maps and DM soliton parameters in dimensionless units. The typical power is $P_0 = 2$ mW, the typical nonlinear length is $Z_0 = 250$ km, and the typical time is $T_0 = 5$ ps.

	l_+	l_-	d_+	d_-	d_m	C_E	$T_{rms\text{DM}}$	$T_{rms\text{theo}}$	$\max(\|u\|^2)_{\text{DM}}$	$\max(\|u\|^2)_{\text{theo}}$
E	0.1	0.1	100	-100	-0.05	1	0.7711	0.7050	0.8793	1.0030
F	0.1	0.1	200	-200	-0.05	1	1.1852	1.0949	0.5771	0.6458